Ship-in-Bottle synthesis of Pt_9-Pt_{15} carbonyl clusters inside NaY and NaX zeolites, in-situ FTIR and EXAFS characterization and the catalytic behaviors in ^{13}CO exchange reaction and NO reduction by CO

Guang-Jin Li *, Toshiyuki Fujimoto, Atsushi Fukuoka and Masaru Ichikawa **

Catalysis Research Center, Hokkaido University, Sapporo 060, Japan

$[Pt_9(CO)_{18}]^{2-}$/NaY (orange-brown, 2056 and 1798 cm^{-1}), $[Pt_{12}(CO)_{24}]^{2-}$/NaY (dark-green, 2080 and 1824 cm^{-1} and $[Pt_{15}(CO)_{30}]^{2-}$/NaX (yellow-green, 2100 and 1865 cm^{-1}) were stoichiometrically synthesized by the reductive carbonylation of $[Pt(NH_3)_4]^{2+}$/NaY, Pt^{2+}/NaY and Pt^{2+}/NaX, respectively. The IR bands characteristic of their linear carbonyls shift to higher frequencies whereas the bridging CO bands to lower frequencies, compared with those on the external zeolites and in solution. In-situ FTIR studies suggested that the subcarbonyl species such as PtO(CO) and "$Pt_3(CO)_3(\mu_2-CO)_3$" are formed as the proposed intermediates towards $[Pt_{12}(CO)_{24}]^{2-}$/NaY in the reductive carbonylation of Pt^{2+}/NaY. ^{13}CO exchange reaction preceded with the different intrazeolite Pt carbonyl species in the following order of activity at 298–343 K: "$Pt_3(CO)_3(\mu_2-CO)_3$"/NaY $\gg$ PtO(CO)/NaY $>$ $[Pt_9(CO)_{18}]^{2-}$/NaY $>$ $[Pt_{12}(CO)_{24}]^{2-}$/NaY. Pt-L_3-edge EXAFS measurment for these synthesized samples demonstrated that they are consistent with the Pt carbonyl clusters having trigonal prismatic Pt_9 and Pt_{12} frameworks infered to a series of the Chini complexes such as $[NEt_4]_2[Pt_3(CO)_6]_n$ ($n = 3$–5). The intrazeolite Pt_9 and Pt_{12} carbonyl clusters exhibited higher cataytic activity in NO reduction by CO towards N_2 and N_2O at 473 K, compared with those on the conventional Pt/Al_2O_3 catalysts. The mechanism of intrazeolite Pt_9-Pt_{15} carbonyl cluster formation are discussed in terms of the intrazeolite basicity and acidity.

Keywords: Ship-in-Bottle synthesis; Pt carbonyl clusters; NaY zeolites; EXAFS; ^{13}CO exchange; NO + CO reaction

1. Introduction

Widespread interest has recently focused on the surface-grafted metal carbonyl clusters such as $Rh_6(CO)_{16}$, $[Rh_4Fe_2(CO)_{15}]^{2-}$ [1], $[Pt_3(CO)_6]_n^{2-}$ ($n = 3, 5$)

---

* On leave from National Laboratory for Catalysis, Dalian Institute of Chemical Physics, Chinese Academy of Sciences, Dalian, 129 Street, China.

** To whom all the correspondence should be addressed.

[4,5] and $Os_3(CO)_{12}$ [6] on SiO_2, Al_2O_3 and MgO. They may offer many advantages for molecular approaches in rational preparation of the tailored metal catalysts [1–3]. Removing ligands of surface-bound organometallics can result in active metal/alloy particles having uniform sizes and discrete metal compositions. Generally, under the catalytic reaction conditions, e.g., higher temperature and pressures, the surface-bound metal clusters are difficult to maintain their original cluster structures and easy to be collapsed to give the relatively larger metal particles. Among different kinds of inorganic supports, zeolites (especially X and Y type) are most suitable to entrap the metal/alloy clusters to prevent cluster sintering. In addition, zeolites are aluminosilicate crystallines consisting of pore structure of molecular dimensions (8–13 Å), interconnected with smaller windows (5–8 Å diameter). The intrazeolite circumstances alike "solid-solvent" can accomodate selected organic and inorganic molecules, even metal complexes such as Fe phthalocyanine [7], and promote the chemical reactions, similarly in solution. Zeolite supercages can supply "template" circumstances for the synthesis of metal clusters to fit the interior supercages by means of so-called "ship-in-bottle" technique [8]. The tailored metal catalysts can be derived from the zeolite encapsulated metal carbonyl clusters. Some intrazeolite metal carbonyl clusters $Rh_6(CO)_{16}$ [3,9], $Ir_6(CO)_{16}$ [10,14], $Pd_{13}(CO)_x$ [11], $[HFe_3(CO)_{11}]^-$ [12], $[Fe_2Rh_4(CO)_{16}]^{2-}$ [13] and $Rh_{6-x}Ir_x(CO)_{16}$ ($x = 2, 3, 4$) [1,14] were previously synthesized and characterized. The catalysts derived from $Pd_{13}(CO)_x$/NaY [15] and $Rh_6(CO)_{16}$/NaY [16] showed unique catalytic performances in $CO + H_2$ and olefin hydroformylation reactions based on their molecular shape-selectivity.

We report here that various Pt carbonyl clusters having general formula $[Pt_3(CO)_3(\mu_2-CO)_3]_n^{2-}$ ($n = 3$–5) are synthesized in NaY and NaX zeolites which were characterized by FTIR, UV-vis and EXAFS spectroscopies. The mechanism of the Pt carbonyl cluster formation was studied by in-situ FTIR, and it was proposed that $[Pt_3(CO)_3(\mu_2-CO)_3]$ and PtO(CO) are as intermediates towards $[Pt_{12}(CO)_{24}]^{2-}$/NaY in the reductive carbonylation of Pt^{2+}/NaY. ^{13}CO exchange reaction and NO reduction by CO were conducted on the intrazeolite Pt_9 and Pt_{12} carbonyl clusters.

2. Experimental

$[Pt(NH_3)_4]^{2+}$/NaY and $[Pt(NH_3)_4]^{2+}$/NaX (4.0 Pt wt% loading) were prepared by cation-exchange of NaY (Linde LZY-52, Lot No. 030785, Si/Al = 5.6, surface area 910 m^2/g) and NaX powder (Union Showa K.K. 13X, Lot No. 980113, Si/Al = 2.3, surface area 870 m^2/g) with $[Pt(NH_3)_4]Cl_2$, respectively. During stirring of the zeolite slurry, the aqueous solution of $[Pt(NH_3)_4]Cl_2$ was added in drops (2.6 mM, PH = 8.90) followed with stirring at 298 K for 24 hrs. After filtering and washing by deionized water, the samples were dried at 393 K.

$[Pt(NH_3)_4]^{2+}$/NaY(X) was calcined in O_2 flow (120 ml/min) at 573 K for 2 hrs (0.5°C/min) to give Pt^{2+}/NaY and Pt^{2+}/NaX. Most of the Pt in the grey-black oxidized sample is located in the supercages of NaY or NaX with a bivalent form Pt^{2+} as reported by P. Gallezot et al. from TPR results [17].

The reductive carbonylation of $[Pt(NH_3)_4]^{2+}$/NaY, Pt^{2+}/NaY and Pt^{2+}/NaX were carried out in a Pyrex-glass reactor under CO (400–760 Torr) at 298–373 K after the samples were evacuated at 353 K for 2 hrs. A small amount of water was added to the calcined Pt^{2+}/NaY and Pt^{2+}/NaX to promote the reductive carbonylation with CO.

IR spectra were recorded on a Shimadzu FTIR-4100 double beam spectrometer with 25–100 time scans at resolution 2 cm^{-1}. Each sample was pressed into a self-supporting wafer (8 mg/cm^2) and mounted in a quartz IR cell. The in-situ IR measurements were conducted to monitor the reductive carbonylation of the Pt ion-exchanged zeolite samples by flowing gases of CO, H_2, NO and H_2O.

The reflectant UV-vis spectra of powder samples were recorded by using a Hitachi 330 UV-vis spectrometer.

^{13}CO isotopic exchange reactions were studied in the IR cell under 20–50 Torr of ^{13}CO (98% ^{13}CO enriched) purchased from Merck Reagent Co., Ltd..

EXAFS measurments were carried out at SOR beam line 10B of the Photon Factory in the National Laboratory for High Energy Physics (KEK-PF) using synchrotron radiation with an electron energy of 2.5 GeV at currents of 100–250 mA. The EXAFS and XANES spectra were measured at the L_3 edge of Pt (11562 eV) using a Si(111) double crystal monochromator. The sample wafers were stored under Ar or CO gases in specially designed Pyrex-glass cells with Kapton film windows (500 nm thick). Pt foil and $[Pt_{12}(CO)_{24}][NEt_4]_2$ mixed with BN (Boron Nitride) were chosen as references. $[Pt_{12}(CO)_{24}][NEt_4]_2$ crystal was synthesized according to literature methods [18] and purified by several recrystalizations which was identified by the characteristic IR bands of its THF solution at 2046(vs), 1882(w), 1863(s) and 1832(w) cm^{-1}. The analysis of EXAFS data were derived using the computer program "PROGRAM 2" by Fourier-Transform curve-fitting method, as described elsewhere [19].

CO + NO reaction was performed at reduced pressure ($P_{CO} = 50$ Torr, $P_{NO} = 50$ Torr) in a closed circulating Pyrex-glass reaction system. The products were analyzed by on-line TCD gas-chromatography (Shimadzu GC-8A) using 5A molecular sieves (60 cm-long) and Porapak Q (3 m-long) columns for CO, NO, N_2O, N_2 and CO_2 with helium as carrier gas (30 ml/min).

3. Results and discussion

3.1. SYNTHESIS OF $[Pt_9(CO)_{18}]^{2-}$/NaY

The in-situ FTIR observation was performed in CO reaction with $[Pt(NH_3)_4]^{2+}$/NaY after evacuation at 353 K for 2 hrs (fig. 1a). When 400 Torr

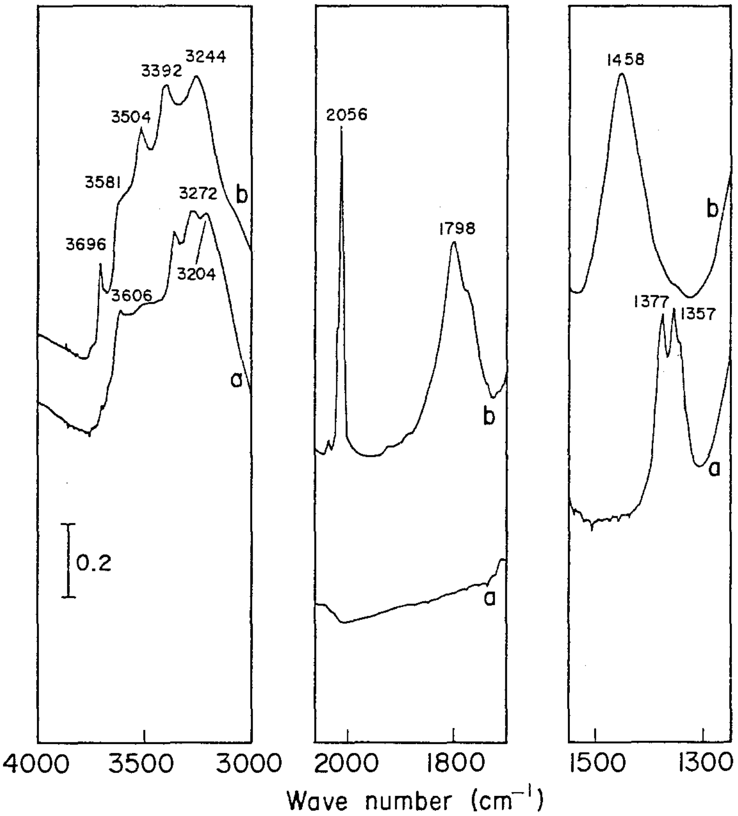

Fig. 1. IR spectra of $[Pt(NH_3)_4]^{2+}/NaY$ in the reductive carbonylation. (a) $[Pt(NH_3)_4]^{2+}/NaY$ (4 wt% Pt loading) after evacuation at 353 K for 2 hrs; (b) After heating at 373 K under 500–760 Torr CO for 20 hrs.

of CO was admitted onto the $[Pt(NH_3)_4]^{2+}/NaY$ wafer in the IR cell at 373 K, the sample became pink and showed the weak IR bands at 1798, 1836, 1898, 2086 cm^{-1}, similarly as reported by A. De Mallmann et al. [20]. After further heating at 373 K under the CO atmosphere, the sample changed to orange-brown and two sharp and intense CO bands at 2056 and 1798 cm^{-1} were developed as shown in fig. 1b, accompanied by CO_2 formation in gas phase. The intense bands both in linear CO and bridging CO region are similar to those of the Pt carbonyl clusters synthesized in solution and the color of the sample resembles that of $[Pt_9(CO)_{18}]^{2-}$ in THF solution (violet-red) [18]. The orange-brown species is proposed to be $[Pt_9(CO)_{18}]^{2-}$ located in NaY zeolites. It is interesting to find that during the reductive carbonylation of $[Pt(NH_3)_4]^{2+}/NaY$ the coordinated NH_3 (3350, 3270, 3208 cm^{-1} due to N-H stretching and 1357, 1377 cm^{-1} due to NH_3 deformation) (fig. 1a) are completely converted into NH_4^+ adsorbed on NaY characteristic of the IR bands at 3392, 3344 cm^{-1} (N-H) and 1458 cm^{-1} (deformation) [21]. This suggested that the Pt-coordinated NH_3 has reacted with water by heating at 300–373 K to give a basic OH^- and NH_4^+ which is bound with the intrazeolite $[Pt_9(CO)_{18}]^{2-}$ as the counter-cations. A basic OH^- generated inside NaY cavity may promote the formation of the Pt carbonyl cluster anions, similarly the synthesis in solution [18]. Accordingly, it is suggested that the reductive carbonylation of Pt^{2+}/NaY towards $[Pt_9(CO)_{18}]^{2-}$/NaY proceeds as follows:

$$9\ Pt(NH_3)_4^{2+}/NaY + 28\ CO + 26\ H_2O \rightarrow$$

$$[Pt_9(CO)_{18}]^{2-}/NaY + 10\ CO_2 + 36\ NH_4^+/NaY + 16\ OH^-/NaY.$$

3.2. SYNTHESIS OF $[Pt_{12}(CO)_{24}]^{2-}$/NaY AND $[Pt_{15}(CO)_{30}]^{2-}$/NaX

Fig. 2 shows the in-situ FTIR spectra in the reaction of Pt^{2+}/NaY with 550 Torr CO at 298–373 K. Upon the exposure to CO at 298 K, the sharp CO bands appear at 2112(l), 1896(b) and 1841(b) cm^{-1} (species [A]). After these three bands reached their maxima under heating at 353–373 K, new bands at 2080(l) and 1824 cm^{-1} (b) were remarkably developed at the expense of decreasing those due to intermediate species [A]. In 6–10 hrs by heating at 373 K the 2080 and 1824 cm^{-1} bands successively increased and the sample became dark-green (290, 445 and 640 nm in UV-vis spectrum) whereas the species [A] disappeared. Similarly in the formation of $[Pt_9(CO)_{18}]^{2-}$/NaY, this dark-green species is assigned to $[Pt_{12}(CO)_{24}]^{2-}$/NaY which exhibits the IR bands and UV-vis spectra resembling those of the $[Pt_{12}(CO)_{24}]^{2-}$ dianion cluster synthesized in solution [18]. The blue shift of linear CO IR frequency (26–40 cm^{-1}) and red shift of bridging CO frequency (−40–50 cm^{-1}) were observed for $[Pt_{12}(CO)_{24}]^{2-}$/NaY and $[Pt_9(CO)_{18}]^{2-}$/NaY respectively. On the contrary, no appreciable CO frequency shifts were observed when $[Pt_{12}(CO)_{24}][NEt_4]_2$ was deposited from THF solution on the NaY wafer. The CO frequency shifts of the intra-zeolite Pt_9 and Pt_{12} carbonyl clusters is explained by the interaction between O-ended carbonyl in the Pt carbonyl clusters and the acid sites in NaY zeolites, similarly for $[Rh_6(CO)_{16}]$/NaY [3,14]. When the prepared $[Pt_{12}(CO)_{24}]^{2-}$/NaY was washed by MeOH solution of tetraethylammonium chloride $[NEt_4]Cl$, no colored elutant was observed and no CO IR bands appear on the spectrum of the solution. This suggested the $[Pt_{12}(CO)_{24}]^{2-}$/NaY is formed completely inside NaY with a negligible formation on the external surface of zeolite.

After the sufficient removal of water from the Pt^{2+}/NaY by evacuation at 573 K for 2 hrs, it is of interest to find that a new carbonyl species (dark-grey) different from the dark-green $[Pt_{12}(CO)_{24}]^{2-}$/NaY was produced by the reaction of CO + H_2 (250 Torr CO and 250 Torr H_2) at 300–373 K (see in 3.5). Considering the promotion effect with water and the CO_2 formation during the synthesis of $[Pt_{12}(CO)_{24}]^{2-}$/NaY from Pt^{2+}/NaY with CO, the overall reaction

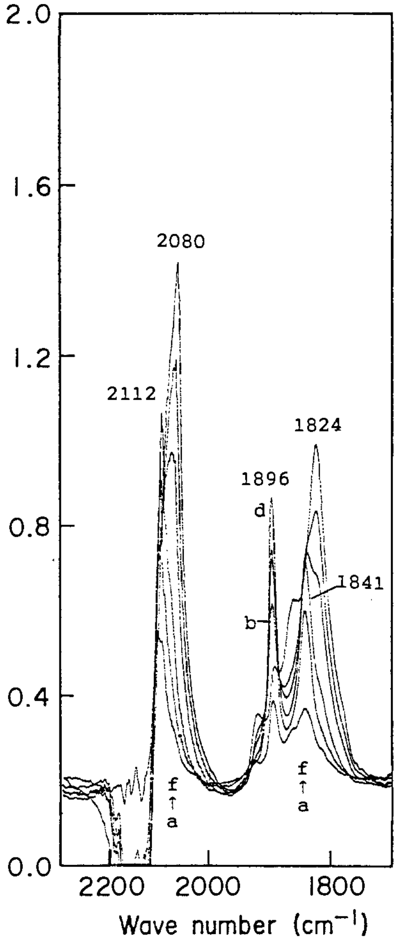

Fig. 2. In-situ FT IR spectra of reductive carbonylation of Pt^{2+}/NaY by 550 Torr CO (with trace amount of H_2O) during heating at 298–353 K. a) 298 K, 20 mins; b) 353 K, 3 mins; c) 353 K, 10 mins; d) 353 K, 1 hr 30 mins; e) 353 K, 3 hrs; f) 353 K, 7 hrs.

is proposed to consist of the following reductive carbonylation:

$$12\,Pt^{2+}/NaY + 37\,CO + 13\,H_2O \rightarrow$$
$$[Pt_{12}(CO)_{24}]^{2-}/NaY + 13\,CO_2 + 26\,H^+/NaY.$$

The generated protons may be interacted with $[Pt_{12}(CO)_{24}]^{2-}$ to be accomodated inside NaY cavity. The sizes of the Pt carbonyl cluster dianions formed inside zeolite depend on the interior basicity of $[Pt(NH_3)_4]^{2+}$/NaY and Pt^{2+}/NaY, similarly as the trends of oligomerization of trigonal prismatic Pt carbonyl cluster anions synthesized in the reductive carbonylation of H_2PtCl_6 (or $Pt(CO)_2Cl_2$) in alkaline methanol solution. Chini et. al. [18] reported that by increasing the basicity (OH^- concentration) of solution the smaller Pt carbonyl clusters such as $[Pt_9(CO)_{18}]^{2-}$ and $[Pt_6(CO)_{12}]^{2-}$ are obtained.

The reductive carbonylation of Pt^{2+}/NaX gave a yellow-green species characteristic of the CO IR bands at 2100(l) and 1865(b) cm^{-1}. This carbonyl species was also proposed to be assigned to $[Pt_{15}(CO)_{30}]^{2-}$ inside NaX in terms of the characteristic CO IR bands and color which corresponds to the molecular Pt_{15} carbonyl cluster dianion in THF solution.

3.3. EXAFS CHARACTERIZATION

To obtain more insight into the structures of Pt carbonyl clusters formed in NaY zeolites, the EXAFS (Extended X-ray Absorption Fine Structure) spectra of Pt-L_3-edge were measured for the samples of $[Pt_9(CO)_{18}]^{2-}$/NaY and $[Pt_{12}(CO)_{24}]^{2-}$/NaY under N_2 atmosphere at 300 K. The Pt foil and $[Pt_{12}(CO)_{24}][NEt_4]_2$ crystal mixed with Boron Nitride (BN) were used as the references for Pt-Pt and Pt-CO shell. The raw EXAFS data and associated Fourier transforms of the product formed in the reductive carbonylation of $[Pt(NH_3)_4]^{2+}$/NaY and the $[Pt_{12}(CO)_{24}][NEt_4]_2$ crystal mixed with Boron Nitride (BN) is shown in figs. 3, 4. And the results of the curve-fitting analysis are listed in table 1. In the Fourier transforms, main intense peaks around 2–3 Å (before phase-shift correction) and weaker peak at 3.5–4 Å (before phase-shift correction) are possibly assigned to the Pt-Pt bonds in the three different configurations in the Pt cluster frameworks, e.g., an intratriangular(Pt-Pt^a), an intertriangular layer(Pt-Pt^b) and a second neighbored atoms inter-triangle(Pt-Pt^c). For the exclusion of overlapped CO shell contributions, $k > 6.5$ $Å^{-1}$ is used for curve fitting analysis, because C and O contributions are relatively smaller at k greater than 6.5 $Å^{-1}$. The crystal structure by X-ray diffraction analysis by Dahal et al. [22], provides the data for the Pt-Pt coordination: $C.N._{Pt\text{-}Pt^a} = 2$, $R = 2.66$ Å; $C.N._{Pt\text{-}Pt^b} = 1.5–1.3$, $R = 3.05$ Å and $C.N._{Pt\text{-}Pt^c} = 3–2.5$, $R = 4.04$ Å for $[Pt_9(CO)_{18}]^{2-}$ and $[Pt_{15}(CO)_{30}]^{2-}$, respectively. With these parameters, a best estimate for the Pt-Pt shell was calculated. A Debye-Waller factor of 0.04–0.09 (relative to Pt foil) was determined, which gave the best agreement with the EXAFS data in r space 2.0–3.0 Å (before the phase-shift correction) for $R_{Pt\text{-}Pt^a}$ and $R_{Pt\text{-}Pt^b}$ and 3.6–3.8 Å (before the phase-shift correction) for $R_{Pt\text{-}Pt^c}$.

After substraction of the calculated Pt-Pt contribution for the experimental results, a Fourier transform was again applied, with a k^3 weighting used to separate the Pt-C and Pt-O peaks in r space with $r = 1.2–3.4$ Å to give a Pt-CO reference. The backtransformation spectrum is taken to be reliable as an Pt-CO reference only between $k = 4–14$ $Å^{-1}$. Using the value for $C.N.$ and the distances $R_{Pt\text{-}C}$ and $R_{Pt\text{-}O}$ equal to the values characteristic of the uncapsulated parent cluster, $[Pt_{12}(CO)_{24}][NEt_4]_2$: $R_{Pt\text{-}C} = 2.05$ Å, $C.N. = 2.0$ and $R_{Pt\text{-}O} = 3.32$ Å, $C.N. = 1.0$, the EXAFS for a Pt-CO shell was calculated. A Debye-Waller factor was found to give the best curve-fittings of EXAFS oscillation in r space, 1.6–1.8 Å for Pt-C and 2.9–3.1 Å for Pt-O. The experimental results on the

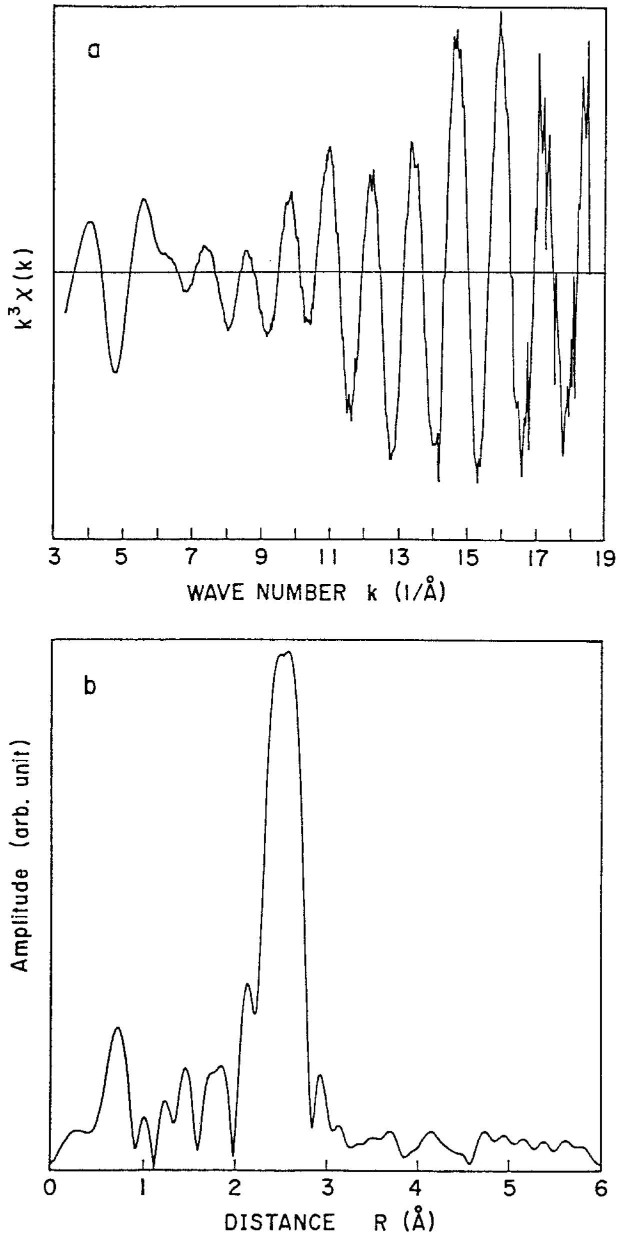

Fig. 3. Pt L_3-edge EXAFS data for $[Pt_9(CO)_{18}]^{2-}$/NaY, (a) k^3-weighted EXAFS oscillation, (b) Associated Fourier transform.

Pt-CO shell for the samples of the yellow-brown $[Pt_9(CO)_{18}]^{2-}$/NaY and the dark-green $[Pt_{12}(CO)_{24}]^{2-}$/NaY are shown in table 1.

The Fourier transforms for the sample of $[Pt_{12}(CO)_{24}]^{2-}$/NaY is very similar to that of the reference $[Pt_{12}(CO)_{24}][NEt_4]_2$/BN. The interatomic distances and

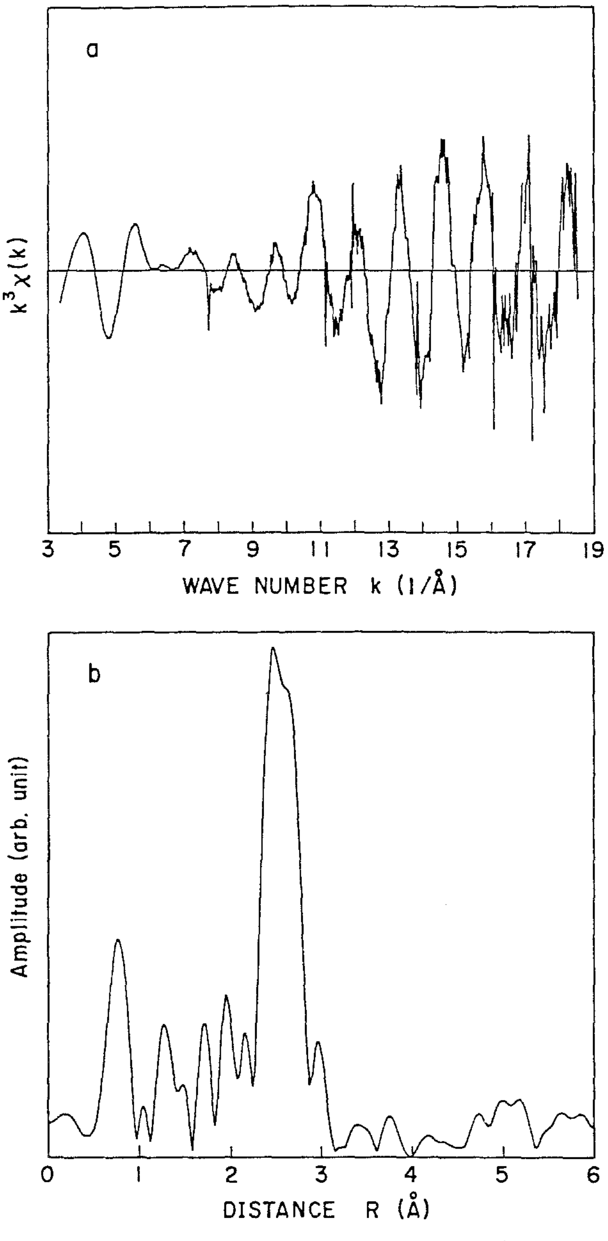

Fig. 4. Pt L_3-edge EXAFS data for $[Pt_{12}(CO)_{24}][NEt_4]_2$/BN, (a) k^3-weighted EXAFS oscillation, (b) Associated Fourier transform.

C.N. of both intratriangular(Pt-Pt[a]) and interlayer bonding(Pt-Pt[b]) are quite consistent between them within the experimental errors ($R = 0.03$ Å, and $C.N. = 0.2$), as shown in table 1. The results suggested that the prismatic triangular Pt clusters like $[Pt_{12}(CO)_{24}]^{2-}$ are most likely formed in the sample which was prepared from Pt^{2+}/NaY in the reductive carbonylation. There is not

Table 1
EXAFS evaluation for Pt_9 and Pt_{12} carbonyl clusters in NaY zeolites and parent Pt_{12} cluster

	$[NEt_4]_2[Pt_{12}(CO)_{24}]$/ BN			$[Pt_{12}(CO)_{24}]^{2-}$/ NaY			$[Pt_9(CO)_{18}]^{2-}$/ NaY			Pt foil		
	R	*C.N.*	σ	*R*	*C.N.*	σ	*R*	*C.N.*	σ	*R*	*C.N.*	σ
Pt-Pt[a]	2.65	2.0	0.05	2.64	1.7	0.04	2.64	1.9	0.04	2.77	12	0.06
Pt-Pt[b]	2.99	1.5	0.08	2.99	1.7	0.09	2.99	1.7	0.09	–	–	–
Pt-Pt[c]	3.88	3.0	0.06	3.87	2.9	0.07	3.85	3.0	0.06	–	–	–
Pt-C[d]	2.05	2.0	0.02	2.05	1.3	0.01	2.06	1.7	0.00	–	–	–
Pt-O[e]	3.32	1.0	0.01	3.28	0.5	0.01	3.28	0.9	0.00	–	–	–

R; Inter atomic distance: *C.N.*; Coordination number: σ; Debye-Waller factor
Estimated experimental errors are ±0.03 Å for atomic distance and ±0.2 for coordination number on the present EXAFS evaluation.
* Pt-Pt[a]; Intra-triangular.: Pt-Pt[b]; Inter-triangular.: Pt-Pt[c]; Second neighbored atoms for inter-triangle.

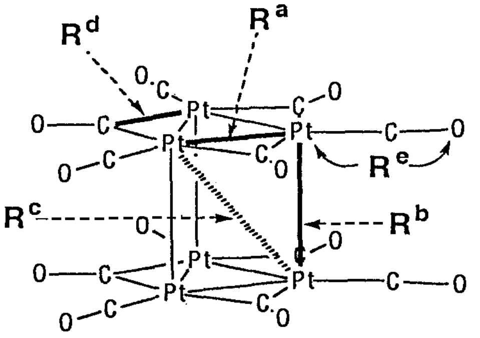

appreciable change in their cluster frameworks between the intrazeolite complex and their parent clusters. The smaller values of the *C.N.* for Pt-C and Pt-O bonding in the Pt_{12} carbonyl cluster dianion inside NaY, compared with those for the parent molecule might be reflected in some structural distortion due to the intrazeolite constraint. The sample of $[Pt_9(CO)_{18}]^{2-}$/NaY gave the EXAFS results similar to those of the sample $[Pt_{12}(CO)_{24}]^{2-}$/NaY and the reference $[Pt_{12}(CO)_{24}][NEt_4]_2$ in terms of *R* and *C.N.*, as shown in table 1, implying the stoichiometric formation of $[Pt_9(CO)_{18}]^{2-}$ cluster in the sample which was prepared by the reaction of CO with $[Pt(NH_3)_4]^{2+}$/NaY.

3.4. ^{13}CO ISOTOPIC EXCHANGE REACTION

The ^{13}CO exchange reaction was conducted on the species [A] 2112(l), 1896(b) and 1841(b) cm^{-1}) formed in the initial stage of the carbonylation of Pt^{2+}/NaY with CO at 298 K. ^{13}CO was very quickly exchanged with the species [A] to give new bands at 2060, 1852 and 1802 cm^{-1} due to ^{13}CO isotopic shift. The reaction proceeds very slowly on $[Pt_{12}(CO)_{24}]^{2-}$/NaY and $[Pt_9(CO)_{18}]^{2-}$/

NaY even at higher temperatures such as 343 K. By the analogy of its bridging CO IR bands with those characteristic of triangular Pt complexes such as $[Pt_3(\mu_2-CO)_3][PPh_3]_4$ (1803(s) and 1788(s) cm^{-1} in Nujol mull) [23], it suggested that species [A] may be an intermediate Pt carbonyls having a similar triangular cluster framework, e.g., "$Pt_3(CO)_3(\mu_2-CO)_3$". The preliminary EXAFS analysis of the proposed intermediate [A) suggests that the sample consists of the isolated triangular Pt-Pt bonds similar to those of the Chini cluster complexes $[Pt_3(CO)_3(\mu_2-CO)_3]_n^{2-}$ ($n=2$–5). ^{13}CO exchange reaction rates were varied on the different intrazeolite Pt carbonyl species in the following order at 298–343 K: $[Pt_3(CO)_3(\mu_2-CO)_3]/NaY \gg [Pt_9(CO)_{18}]^{2-}/NaY > [Pt_{12}(CO)_{24}]^{2-}/NaY$.

3.5. REDUCTIVE CARBONYLATION OF Pt^{2+}/NaY BY $CO+H_2$ MIXED GAS

The reductive carbonylation of Pt^{2+}/NaY proceeds in the presence of water. The water gas shift reaction with $CO+H_2O$ promote the formation of Pt hydride which is incorporated into the successive formation of the Pt carbonyl clusters such as $[Pt_{12}(CO)_{24}]^{2-}/NaY$. When the sample of Pt^{2+}/NaY was evacuated at 573 K for 2 hrs to sufficiently remove water, the dehydrated Pt^{2+}/NaY gave dark-grey complex by reaction with $CO+H_2$ (1 : 1 v/v mixture) of 600 Torr at 300–373 K, showing the IR carbonyl bands at 2110(s), 2088(sh) cm^{-1} for linear CO and 1902(m), 1870(sh), 1850(s), 1800(sh) cm^{-1} for bridging CO. Concerning the carbonyl IR bands as showing in fig. 5 this Pt carbonyl species differs from $[Pt_{12}(CO)_{24}]^{2-}/NaY$, but rather resembles those of $Pd_{13}(CO)_x/NaY$ which was reported by Sachtler et al. [11] to be formed in CO chemisorption of the reduced Pd^{2+}/NaY. The similar carbonyl species was formed in CO chemisorption on the reduced Pt_9/NaY derived from $[Pt_9(CO)_{18}]^{2-}/NaY$, which showed the IR bands at 2104(s), 2090(s) cm^{-1} for linear CO and 1924(m), 1886(sh), 1860(s), 1810(sh) cm^{-1} for bridging CO. The results suggested that Pt^{2+} located in the hexagonal sites of NaY is readily reduced with H_2 to Pt^0 which migrated in the supercage, resulting in the neutral carbonyl cluster like $Pt_{13}(CO)_x$ by aggregation.

3.6. NO INTERACTION WITH $(Pt_{12}(CO)_{24}]^{2-}/NaY$ AND NO+CO REACTION

When NO (150 Torr) was admitted onto the $[Pt_{12}(CO)_{24}]^{2-}/NaY$ (2080 and 1824 cm^{-1}), as shown in fig. 6, it is interesting to find that the intrazeolite Pt_{12} carbonyl dianions substantially decomposed to give the subcarbonyl species; e.g. $[Pt_3(CO)_3(\mu_2-CO)_3]$ (2112, 1896 and 1841 cm^{-1}) [A]. At this stage of the reaction, the active species [A] was nicely differentiated from other carbonyl species by ^{13}CO exchange to give ^{13}CO labelled $[Pt_3(CO)_3(\mu_2-CO)_3]$ (2060, 1852 and 1802 cm^{-1}). N_2O (2236 cm^{-1}) and CO_2 (2353 cm^{-1}) appeared in the gas phase, followed with carbonate formation (1430 cm^{-1} and 1340 cm^{-1}). In

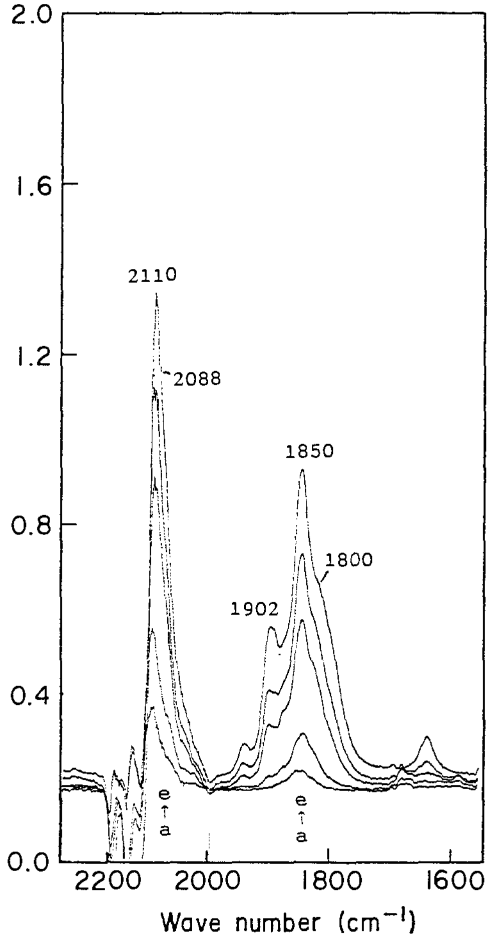

Fig. 5. In-situ IR carbonyl spectra in the reaction of the dehydrated Pt^{2+}/NaY with CO+H_2 (300:300 Torr) at 298–353 K. (a) 298 K, 5 mins; (b) 298 K, 1 hr 30 mins; (c) 353 K, 30 mins; (d) 353 K, 2 hrs; (e) 353 K, 9 hrs.

the further reaction with NO at 298 K for 12 hrs $[Pt_{12}(CO)_{24}]^{2-}$/NaY was completely converted to PtO(CO) (species [B]) having the band at 2110 cm^{-1}. (The similar PtO(CO) species was reported in the coadsorption of CO and O_2 on Pt/Al_2O_3 [24].). The IR bands due to NO adsorbed on Pt are not observed. When the resulting sample was reacted with CO at 353 K, $[Pt_{12}(CO)_{24}]^{2-}$/NaY was regenerated via the reductive carbonylation of species [A] and [B], similarly in the carbonylation of Pt^{2+}/NaY. When the mixture of CO and NO was introduced on the $[Pt_{12}(CO)_{24}]^{2-}$/NaY, N_2O, N_2 and CO_2 were produced at 300–413 K while the intrazeolite Pt_{12} carbonyl cluster keeps its framework. The results suggested that NO reacts with $[Pt_{12}(CO)_{24}]^{2-}$/NaY in breaking into smaller subcarbonyls such as [A] and [B]. The synthesis and cleavage of

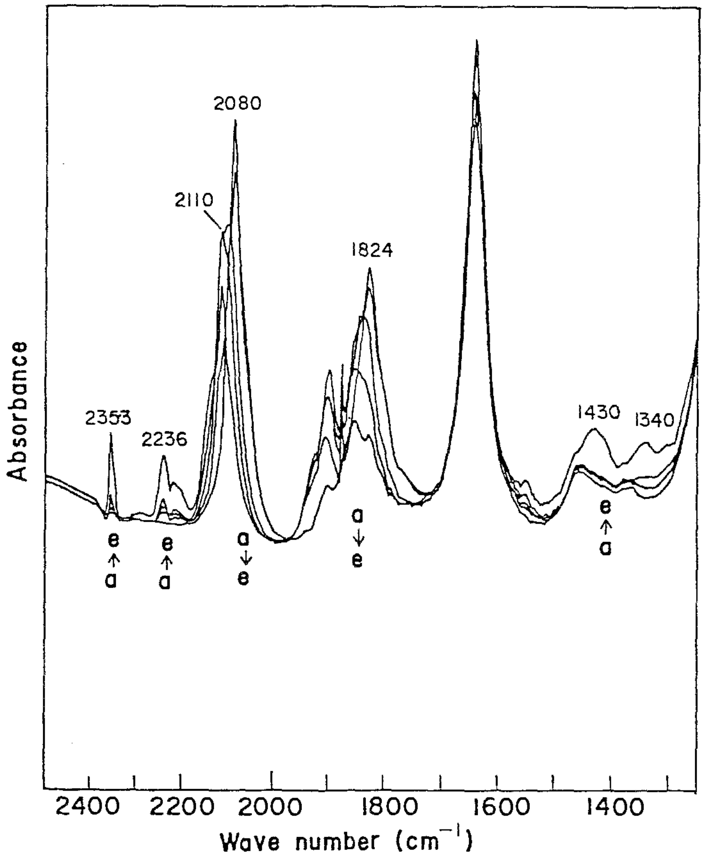

Fig. 6. In-situ FT IR spectra of reaction of $[Pt_{12}(CO)_{24}]^{2-}$/NaY with NO. (a) $[Pt_{12}(CO)_{24}]^{2-}$ (4 wt% Pt)/NaY; (b) admission of 150 Torr NO at 298 K for 1 min; (c) 150 Torr NO at 298 K for 30 mins; (d) 150 Torr NO at 298 K for 1 hr; (e) 150 Torr NO at 198 K for 6 hrs.

$[Pt_{12}(CO)_{24}]^{2-}$ inside NaY proceeds as follows depending on the reaction of CO and NO:

$$Pt^{2+}/NaY \xrightarrow{CO+H_2O} PtO(CO)/NaY \xrightarrow[NO]{CO+H_2O} [Pt_3(CO)_3(\mu_2-CO)_3]$$

$$/NaY \xrightarrow[NO]{CO+H_2O} [Pt_{12}(CO)_{24}]^{2-}/NaY$$

NO reduction by CO was conducted at 473 K on $[Pt_{12}(CO)_{24}]^{2-}$/NaY, $[Pt_9(CO)_{18}]^{2-}$/NaY and Pt/Al_2O_3. As shown in table 2, it is demonstrated that the NaY entrapped Pt_9 and Pt_{12} carbonyl clusters exhibited remarkable activities (10–15 times higher) for formation of N_2O, N_2 and CO_2, compared with those on conventional Pt/Al_2O_3 (4 wt% Pt) catalysts. N_2O was intermediate in CO + NO reaction and successively converts to N_2 in the reaction on Pt_9 and Pt_{12} carbonyl clusters. The conversion of CO + NO reaction and the selectivity towards N_2 were found to be maintained in the steady-state for the prolonged

Table 2
Specific activity for NO+CO reaction at 473 K on NaY-entrapped Pt carbonyl clusters and Pt/Al_2O_3

Catalysts	Catalytic activity in CO-NO reaction		
	NO conversion	N_2 formation	Selectivity
	(10^{-3} molecules Pt^{-1} s^{-1})		$N_2/(N_2+N_2O)$
$[Pt_{12}(CO)_{24}]^{2-}/NaY$	2.00	0.56	0.56
$[Pt_9(CO)_{18}]^{2-}/NaY$	2.83	0.68	0.48
Pt/Al_2O_3	0.58	0.05	0.15

Initial pressure: $P_{NO} = 50$ Torr $P_{CO} = 50$ Torr

on-stream reactions of NO + CO (40 hrs) on these NaY zeolite entrapped Pt_9 and Pt_{12} catalyst samples.

4. Conclusion

1. The reductive carbonylation of $[Pt(NH_3)_4]^{2+}/NaY$ by CO (and H_2O) results in the uniform formation of orange-brown $[Pt_9(CO)_{18}]^{2-}/NaY$ (2056 and 1798 cm^{-1}).

2. Dark-green Pt carbonyl cluster $[Pt_{12}(CO)_{24}]^{2-}/NaY$ is synthesized by the reaction between Pt^{2+}/NaY and CO with a trace amount of water. It gives characteristic IR bands at 2080 and 1824 cm^{-1}.

3. EXAFS results of $[Pt_{12}(CO)_{24}]^{2-}/NaY$ and $[Pt_9(CO)_{18}]^{2-}/NaY$ suggested that the Pt_9 and Pt_{12} carbonyl clusters are formed inside NaY zeolites.

4. The subcarbonyl species such as PtO(CO) (species [B], 2110 cm^{-1}) and "$Pt_3(CO)_3(\mu_2\text{-}CO)_3$" (species [A], 2112, 1896 and 1841 cm^{-1}) are formed as the proposed intermediates towards $[Pt_{12}(CO)_{24}]^{2-}/NaY$. Species [A] exchanges with ^{13}CO very quickly at 298 K, while the Pt_9 and Pt_{12} carbonyl cluster anions inside NaY showed much lower activity in ^{13}CO exchange reaction.

5. H_2 and CO react with Pt^{2+}/NaY to give a Pt carbonyl species which show the IR carbonyl bands at 2110(s), 2088(sh), 1902(m), 1870(sh), 1850(s) and 1800(sh) cm^{-1}, different from those of $[Pt_{12}(CO)_{24}]^{2-}/NaY$, rather resembles $[Pd_{13}(CO)_x]/NaY$ reported by Sachtler et al.

6. NO breaks Pt-Pt bonding in the $[Pt_{12}(CO)_{24}]^{2-}/NaY$ to give Pt subcarbonyls such as [A] and [B]. $[Pt_{12}(CO)_{24}]^{2-}/NaY$ and $[Pt_9(CO)_{18}]^{2-}/NaY$ exhibited the marked activity for the NO reduction by CO towards N_2 and N_2O.

Acknowledgement

A part of this work was financially supported by Grant-in-aid of Ministry of Education, Promotion of Science and Culture (No. 02640330, (C), 1990).

References

[1] M. Ichikawa, in: *Tailored Metal Catalysis*, ed. I. Iwasawa (Reidel, Dordrecht, 1984) 183–263.

[2] M. Ichikawa, L.F. Rao, T. Kimura and A. Fukuoka, J. Mol. Catal. 62 (1990) 15.

[3] L.F. Rao, A. Fukuoka, N. Kosugi and M. Ichikawa, J. Phys. Chem. 94 (1990) 5317.

[4] M. Ichikawa, Chem. Lett. (1976) 335.

[5] J. Puga, R. Patrini, K.M. Sanchez and B.C. Gates, Inorg. Chem. 30 (1991) 2479.

[6] F.B.M. Duivenvoorden, D.C. Koningsberger, Y.S. Uh and B.C. Gates, J. Am. Chem. Soc. 108 (1986) 6254.

[7] N. Herron, G.D. Stucky and C.A. Tolman, J. Chem. Soc., Chem. Commun. (1986) 1521.

[8] J.H. Lunsford, ACS Symp. Ser. 40 (1977) 473.

[9] P. Gelin, Y. Ben Tearit and C. Naccache, J. Catal. 59 (1979) 357.

[10] G. Bergeret, P. Gallezot and F. Lefebure, Stud. Surf. Sci. Catal. 28 (1986) 401.

[11] L.L. Shen, H. Knozinger and W.M.H. Sachtler, Catal. Lett. 2 (1989) 129.

[12] M. Iwamoto and S. Kagawa, J. Phys. Chem. 90 (1986) 5244.

[13] A. Fukuoka, L.F. Rao, N. Kozugi, H. Kuroda and M. Ichikawa, Appl. Catal. 50 (1989) 295.

[14] M. Ichikawa, L.F. Rao, T. Ito and A.F. Fukuoka, Faraday Discuss., Chem. Soc. 87 (1989) 232.

[15] F.A.P. Cavalcanti, C. Dossi, L.L. Sheu and W.M.H. Sachtler, Catal. Lett. 6 (1990) 289.

[16] L.F. Rao, A. Fukuoka and M. Ichikawa, J. Chem. Soc., Chem. Commun. (1988) 13.

[17] P. Gallezot, A. Alarlon-Diaz, J.A. Dalmon, A.J. Renouprez and B. Imelik, J. Catal. 39 (1975) 334.

[18] G. Longoni and P. Chini, J. Amer. Chem. Soc. 98 (1976) 7225.

[19] N. Kosugi and H. Kuroda, Program EXAFS-1, Research Center for Spectrochemistry, The University of Tokyo, 1985.

[20] A. De Mallmann and D. Barthomeuf, Catal. Lett. 5 (1990) 293.

[21] a) J.B. Uytterhoeven, L.G. Christner and W.K. Hall, J. Phys. Chem. 69 (1965) 2117;
b) R.A. Dalla and M. Boudart, in: *Proc. 5th Int. Congr. on Catalysis*, ed. J.W. Hightower (North-Holland, Amsterdam, 1973) 1329.

[22] J.C. Calabrese, L.F. Dahl, P. Chini, G. Longoni and S. Martinengo, J. Am. Chem. Soc. 96 (1974) 2614.

[23] J. Chatt and P. Chini, J. Chem. Soc. (A) (1970) 1538.

[24] M. Primet, J. Catal. 88 (1984) 273.